Final report – Exploration of Enological Raman Spectroscopy Modeling and Analysis

Summary: Raman spectroscopy is a widely applied tool across several industries including textiles, pharmaceuticals, cosmetics, and homeland security, to name but a few. Despite its analytical utility, it has yet to be a widely adopted to across the wine industry. Due to this absence of reference, this primary goal of this work was to establish a baseline for both the strengths as well of the weaknesses of enological Raman analysis. A common problem with traditional or spontaneous Raman spectroscopy as it is commonly referred to is background fluorescence. As Raman spectroscopy obtains the Raman signal by means of laser excitation, the much more efficient fluorescent emission process can easily overtake the more subtle Raman signal if fluorophores such as anthocyanins found in red wines are present in the sample. Initially, it was hypothesized that fluorescence emission in each wine sample would remain constant throughout the life span of the wine and any predictive models could compensate for this baseline loss mathematically. Unfortunately, this was not the case. Over time, fluorescence emission increased over time in the red wine most likely due to the formation of polymeric pigments. This increasing baseline loss was finally resolved by extracting all phenolic compounds in the wine using polyvinylpolypyrrolidone (PVPP). With the application of PVPP, Raman spectral baseline was recovered without sacrificing the predictive power of ethanol and simple sugar predictive models in the wine. After exhaustive inquiry, it was determined that spontaneous Raman spectroscopy can greatly facilitate fermentation monitoring due to its ease of use, analytical speed, and reproducibility.

Title:

Principal Investigator: James Harbertson, Associate Professor, Washington State University.

Christopher Beaver, Associate in Research, Washington State University

Outreach: Poster displayed at Washington Winegrowers in 2021. Open access article published in MDPI Beverages journal in December of 2021: Alcoholic Fermentation Monitoring and pH Prediction in Red and White Wine by Combining Spontaneous Raman Spectroscopy and Machine Learning Algorithms. Continued outreach is planned for future but has been curtailed somewhat by COVID restrictions.

Success Statement: This work provides a simple and relatively inexpensive way to monitor alcoholic fermentation of both red and white wine grapes quickly and accurately. The application of Raman spectroscopy to track enological fermentation can not only directly improve the fermentation process by providing more accurate numbers but also indirectly by allowing more time to be applied to other more time-consuming tasks in the fermentation process.

1. Introduction

When a bundle of light bounces of an object, most of the light scatters and changes direction only. This is called elastic light scattering, which is more commonly known as Rayleigh scattering named as such after John William Strutt, 3rd Baron Rayleigh of Great Britain who discovered the phenomena in 1873 [1]. There is about a one in one million chance, however, that the light will change both direction and frequency. For example, red light may turn to blue light upon scattering. This is called inelastic light scattering, more commonly referred to as Raman scattering named as such after C.V. Raman who discovered these phenomena in 1928 [2, 3]. Since the discovery of the Raman effect, considerable advancements in technology, such as the invention of lasers [4] have given rise to Raman spectroscopy. Essentially, Raman spectroscopy measures the light scatter pattern an object emits when the object is struck with a

laser beam. Rather than measuring the scattered light that is the same frequency as the initial laser light, Raman spectroscopy measures the scattered light that is a different frequency than the initial laser frequency. Of course, the frequency of the scattered light does not simply change without either emitting or absorbing energy. If energy is absorbed by the object that is struck by the laser, this is referred to as a Stokes shift or Stokes fluorescence so named after its discoverer Sir George Stokes of Ireland [5]. If the energy is absorbed by the scattered light, this is referred to as an anti-Stokes shift. As luck would have it, every molecule is possessed of a unique Raman scatter pattern upon laser excitation, thus making Raman spectroscopy an invaluable tool in a wide range of disciplines including pharmaceuticals [6], protein analysis [7], DNA analysis [8], single cell analysis [9], gemstone identification [10], bone structure analysis [11], and many more.

Developing simple, rapid, and accurate measurement practices is of high importance in any industry including the wine industry. A variety of techniques including chromatographic [12] and spectrophotometric [13] methods are available each with its own advantages and drawbacks. Chromatographic methods, while setting standards in terms of both resolution and accuracy, are simply unrealistic for many industrial applications including wine making. Spectrophotometric techniques such as UV-visible spectroscopy are widely applied across the wine industry, and it was in this area that the current study focused. Rather than repeat what has already been established in UV-visible spectroscopy, this study explored new possibilities in the realm of Raman spectroscopy.

At first glance, the fact that the Raman effect is inherently weak may seem like a disadvantage in terms of chemical analysis. This weakness can be taken advantage of when building models for substances that are in great abundance such as sugars in wine grapes that are ultimately converted

to alcohol during wine fermentation. In this case, the weakness aids in model accuracy as it reduces the amount of spectral interference due to the presence of more dilute compounds in red wine such as phenolics. Of course, any analytical technique has its drawbacks as well as advantages, and Raman is no different. The primary disadvantage of the weaker Raman signal in red wine is the presence of anthocyanins which are the primary cause of color in the wine [13]. Anthocyanins fluoresce upon laser exposure, and hence the much more efficient fluorescent spectra can and does easily mask the more subtle Raman spectra [14]. As one might expect, eliminating the primary cause of the problem will often eliminate the problem as well, and this was certainly the case in this study [15, 16]. By removing the fluorescent compounds from the samples, the Raman spectra of both sugars and alcohol were made clearly visible, and the predictive models built using the cleaned wines were extremely accurate.

Raman spectroscopy has been used in a wide variety of relevant applications to the wine industry including spoilage yeast identification [17], methanol and ethanol identification and quantification [18, 19], glucose identification and quantification [20], beverage adulteration quantification [21], phenolic identification [22, 23], sugar and ethanol quantification [24], beverage aging [25], and wine authentication [26], Raman techniques have scarcely been applied directly to wine making. The goal of this study was twofold:

1. Explore ways in which Raman spectroscopy can monitor alcoholic fermentation of wine grapes, and
2. Address ways in which Raman signal obstruction due to fluorescence might be mitigated.

2. Materials and Methods

2.1 Chemicals

Polyvinylpolypyrrolidone (PVPP) was purchased from Central Industrial Sales (Richland, WA, USA).

2.2. Sample Collection

Fruit for both red (Cabernet Sauvignon) and white (Sauvignon Blanc, Grüner Veltliner, Chardonnay) wine fermentations was collected from commercial and research vineyards in the Columbia Valley of Washington State during the 2020 vintage. All alcoholic fermentations were closely monitored until total reducing sugars were below 0.5 g/L. To build predictive models using the Raman spectra, 15 mL samples were collected from each tank several time per day. For phenolic reduction experiments, samples from vintages ranging from 2015 to 2019 were used. Overall, 514 samples were collected in total.

2.3. Reference Analysis

In terms of reference analysis, 254 alcohol concentrations from finished wines, 287 total sugar, glucose, and fructose concentrations from juice and fermenting wines, and 258 pH values of finished wines were measured and recorded using the Anton Paar Alcolyzer (Anton-Paar, Graz, Austria) the Admeo Y15 Automatic Analyzer (Admeo Inc. CA, USA), and the Mettler Toledo Seven Compact S-230 pH meter (Columbus, OH, USA) respectively. Prior to analysis, each instrument was prepared according to the manufacturer's recommendations.

2.4. Raman analysis

For all Raman analysis the portable B&W Tek i-Raman Plus source (Metrohm group, Herisau, Switzerland) equipped with a 785 nm laser, a cooled charge-coupled detector and a BCR100A accessory for liquid sample quantification was used. Briefly, one milliliter of wine was placed in a cuvette and the Raman spectrum was obtained using the B&W Tek BWSpec 4.11 software.

Recorded spectra consisted of an average of five scans at a 4.5 cm^{-1} resolution at a range of 65 to 3350 cm^{-1}. The acquisition time was between 100 to 8000 milliseconds at a constant laser power of 340 mW.

2.5. Phenolic Reduction

A total of 137 samples were used for PVPP exposure. Briefly, 120 mg of PVPP was added to a 1.5 mL red wine sample was added to a 1.5 mL microcentrifuge tube and vortexed for 10 minutes at 15,000 rotations per minute (rpm). The vortexed samples were then measured using the above-mentioned Raman analysis process.

2.6. Statistical Analysis

All models were built using the R Project for statistical computing (version 4.0.2) and RStudio (version 1.3.1073, release name "Giant Goldenrod"). Prior to model building, all spectral data were scaled using the scale function from the R base package. Next, optimal parameters for cost, number of components, and lambda for support vector regression (SVR), partial least squares regression (PLSR), and ridge regression (RR) respectively were determined. Briefly, the full dataset was randomized by row and divided into training (80 percent) and test (20 percent) sets, and the optimal parameter for each algorithm was determined by running each algorithm through a set of possible parameters for that algorithm. After the optimal parameter for each algorithm was determined, models were trained and validated twenty times.

2.7. Software

Al Raman spectra were obtained using the BWSpec software from B&W Tek (Metrohm group, Herisau, Switzerland). Statistical data was obtained using the R Foundation for Statistical

Computing (Vienna, Austria). SVR was obtained using the e1071 package, PLSR was obtained using the pls package, and RR was obtained using the ridge package.

3. Results and Discussion

3.1. Algorithm Comparison and Feature Selection

In any machine learning analysis, one algorithm is significantly outperforming all others typically points towards some error in sample preparation rather than algorithm strength. For that reason, three common multivariate regression algorithms (SVR, PLSR, and RR) were used to ensure model integrity. As shown in table one, all models performed similarly with no one algorithm outperforming the others exclusively.

Additionally, the Raman spectra can be filtered without sacrificing model integrity due to its high native resolution. For example, different regions of the Raman spectra can be used for ethanol (57:1,796 cm^{-1} and 2803:3362 $cm^{-1)}$ and total sugars (57:847 cm^{-1}) models as suggested by Teixeira et al. [27]. A more general filtration (375:3362 cm^{1}) to compensate for highly fluorescent samples that hit the maximum permitted value cap of the BWSpec software was also applied, although the difference was negligible suggesting mathematical filtration rather than physical filtration is trustworthy.

3.2. Ethanol and Total Sugar Model Performance

Table 1. Summation of raw ethanol, raw pH, PVPP exposed ethanol, PVPP exposed pH, and total sugars model performance.

Algorithm	Ethanol – Raw Spectra		pH – Raw Spectra		Ethanol – Post PVPP Spectra		pH – Post PVPP Spectra		Total Sugars	
	RMSE	R^2	RMSE	R^2	RMSE	R^2	RMSE	R^2	RMSE	R^2
SVR	1.35	0.51	1.16	0.62	0.23	0.98	0.12	0.79	1.59	0.96
PLSR	1.22	0.50	1.17	0.61	0.21	0.99	0.12	0.84	1.57	0.95

RR	1.19	0.50	1.16	0.67	0.23	0.99	0.12	0.82	1.57	0.95

SVR = Support Vector Regression
PLSR = Partial Least Squares Regression
RR = Ridge Regression
RMSEP = Root Mean Squared Error of Prediction
R^2 = Coefficient of Determination.

Table 1 also demonstrates the effectiveness of PVPP filtration for ethanol and pH model performance. Sugar models were built prior to or during red wine fermentation in which case background interference due to the presence of fluorophores was minimal and did not affect model integrity. As shown in figure 1, base line loss due to the presence of anthocyanins in red wine significantly increased after fermentation was complete (Figure (1(c)) as opposed to in white wines (figures 1 (b) and (d)) which have no anthocyanins.

Predictive models for glucose and fructose individually did not perform well, most likely due to excessive spectral overlap between the sugars as described by Pierna et al. [28]. Since total sugars calculates both fructose and glucose combined, the effect of overlapping spectra is negated.

3.2.1. Post Fermentation Baseline Loss

Even though ethanol gives a strong Raman single with a 785 nm laser, background fluorescence due to the presence of anthocyanins and polymeric pigments in red wines either partially or completely mask the Raman spectra of ethanol [29, 30]. This baseline loss can be corrected mathematically in young wines without sacrificing model integrity (Figure 1(c)).

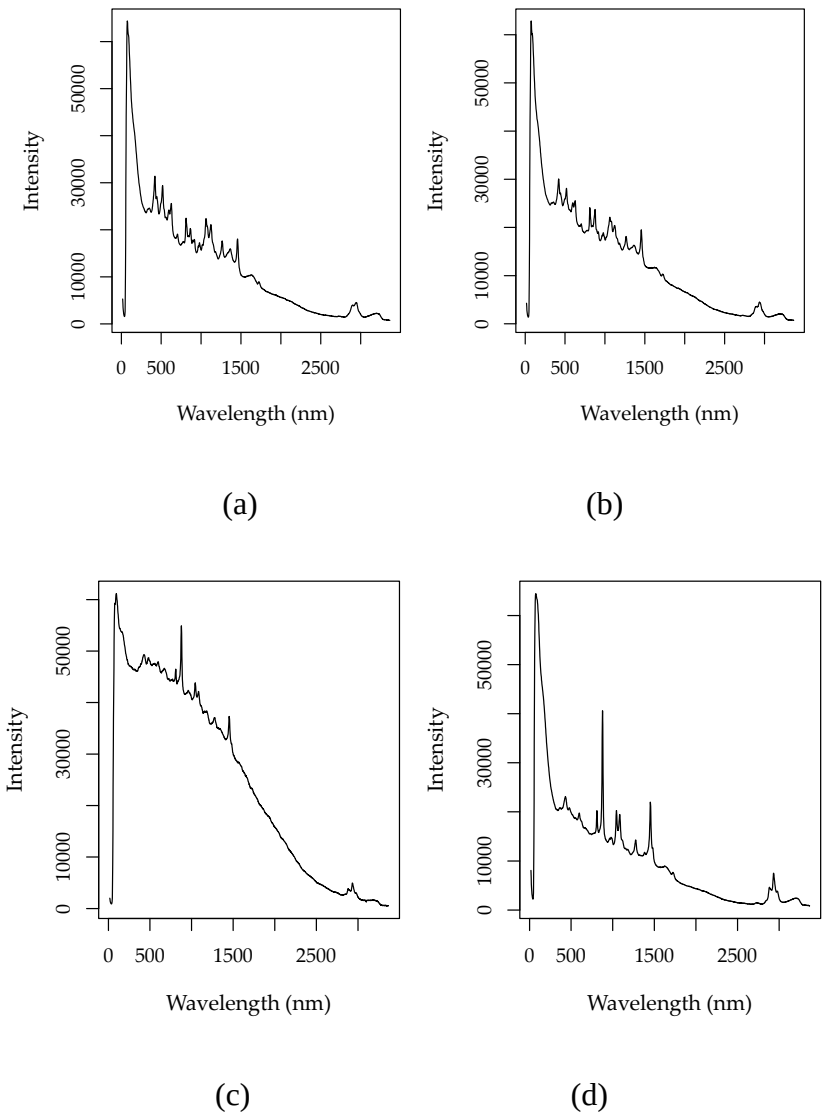

Figure 1. Raman spectra of Cabernet Sauvignon and Chardonnay before fermentation (a, b) and after fermentation (c, d) respectively.

As red wine ages and anthocyanins bond with other molecules and form pigments [31, 32], so to increases the chance of ethanol interacting with the newly formed pigments. As ethanol becomes less physically flexible due to its interactions with pigments through hydrogen bonding, the chances of the molecule emitting a Raman signal decrease since molecular flexibility is crucial to Raman scattering. Additionally, maximum spectral intensities were positively correlated with recorded polymeric pigment (PP) values but very negatively correlated with wine age when laser

exposure time was factored in (R_{PP} = 0.51, $R_{Vintage}$ = - 0.91, data not shown). Summarily, as the wine aged and the red wine phenolics formed pigments, their spectral intensities increased due to fluorescence emission rather than Raman scattering (Figure 2). The decreasing Raman intensity combined with an increasing fluorescence intensity further inhibited Raman peak visibility as well as predictive accuracy.

Although pH measurements are not molecule specific, Raman spectroscopy coupled with machine learning has been suggested as a novel way to obtain pH values nonetheless [33]. Like ethanol, pH measurement accuracy was significantly affected by baseline loss due to fluorescence (Table 1).

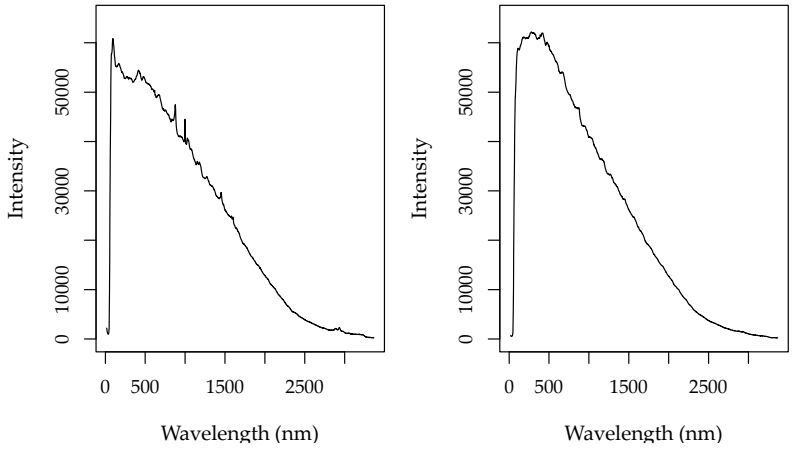

(a) (b)

Figure 2. Comparison of the Raman spectra of a Syrah wine one year after fermentation (a) and five years after fermentation (b).

3.2.2. Fluorescence Reduction using polyvinylpolypyrrolidone (PVPP)

This study demonstrated conclusively that Raman spectroscopy can give very accurate predictions if the samples are first filtered with polyvinylpolypyrrolidone (PVPP) shown in figure 2. As shown in the figure sample exposure to 67 mg/L of PVPP yielded highly accurate predictive models for both ethanol and pH (Table 1).

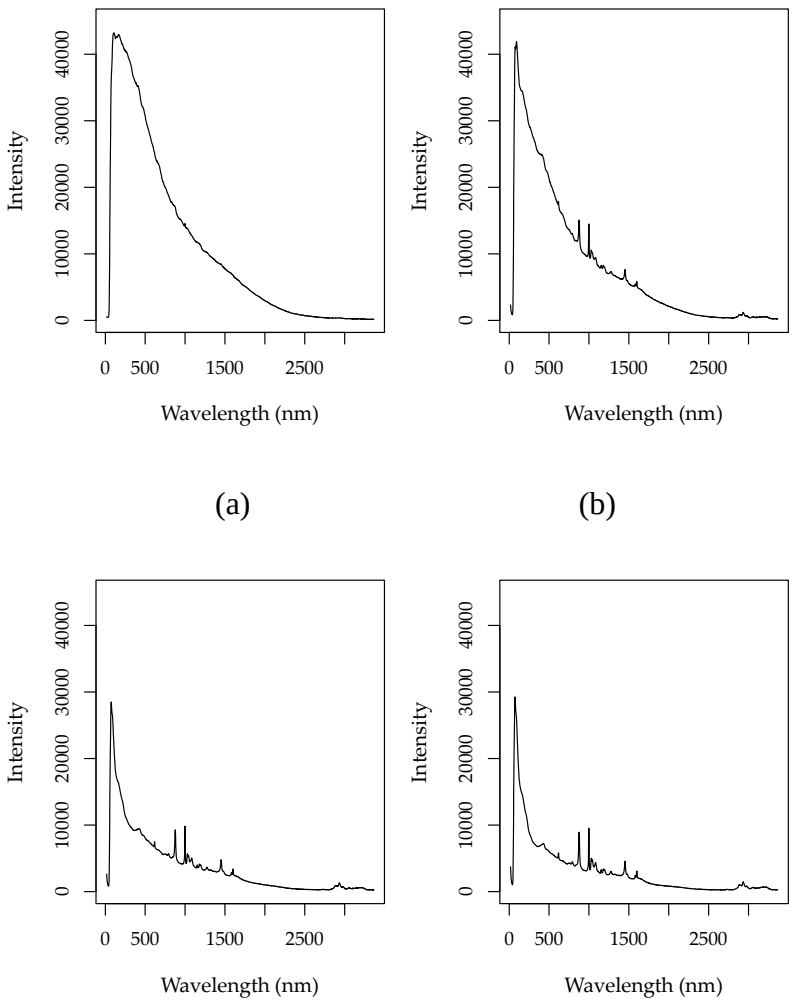

Figure 3. Raman spectra of red wine filtered with 47 mg/L (a), 53 mg/L (b), 60 mg/L (c), and 67 mg/L (d) of polyvinylpolypyrrolidone (PVPP).

5. Conclusions

Predictive models of ethanol, pH, and total sugars in wine using Raman spectroscopy offer a quick and easy alternative to other common analytical methods before, during and after alcoholic fermentation. The weak native signal of spontaneous Raman spectroscopy reduces background interference from other more dilute compounds, and the high native resolution and minimal sample prep needed for Raman spectroscopy make it a very attractive enological fermentation monitoring

tool. Background fluorescence in red wines present a unique challenge in Raman modeling as florescence is a much more efficient process than Raman scattering, not to mention that this fluorescence increases as the wine ages and pigments. Phenolic polymers can easily be removed with polyvinylpolypyrrolidone (PVPP), thus eliminating the background fluorescence issue entirely. In closing, while Raman spectroscopy is widely applied across many industries, Raman spectroscopy for enology is a budding field. Surface-enhanced Raman spectroscopy (SERS), spatially offset Raman spectroscopy (SORS), ultraviolet (UV) Raman spectroscopy, and photoacoustic Raman spectroscopy (PARS) represent only a fraction of the many possible applications of vibrational spectroscopy that have yet to be fully explored in both viticultural and enological applications.

Reference

1. Strutt, J.W. XV. On the light from the sky, its polarization and colour. *The London, Edinburgh, and Dublin Philosophical Magazine and Journal of Science* **1871,** *41***,** 107–120.
2. Banerjee, S. C.V. Raman and colonial physics: Acoustics and the quantum. *Physics in Perspective* **2014**, *16*, 146–78.
3. Raman C.V.; Krishnan K.S. A new type of secondary radiation. *Nature* **1928**, *121*, 501–502.
4. Radziemski, L.; Cremers, D. A Brief history of laser-Induced breakdown spectroscopy: From the concept of atoms to LIBS 2012. *Spectro Acta B* **2013**, *87*, 3–10.
5. Stokes, G.G. On the composition and resolution of streams of polarized light from different sources. *Transactions of the Cambridge Philosophical Society* **1852**, *9*, 399–416.
6. Fini, G. Application of Raman spectroscopy in pharmacy. *J. Raman Spec.* **2004**, *3*, 335-337.
7. Bunaciu, A.A.; Aboul-Enein, H.Y.; Hoang, V.D. Raman spectroscopy for protein analysis. *Applied Spec. Reviews* **2015**, *50*, 377-386.

8. Pyrak, E.; Kajczewski, J.; Kowalik, A.; Kubelski, A.; Jaworska, A. Surface enhanced Raman spectroscopy for DNA biosensors—how far are we? *Molecules* **2019**, *24*, 4423.
9. Strohm, E.M.; Moore, M.J.; Kolios, M.C. High resolution ultrasound and photoacoustic imaging of single cells. *Photoacoustics* **2016**, *4*, 36-42.
10. Jenkins, A.; Larsen, R. Gemstone identification using Raman spectroscopy. *Spectroscopy* **2004,** *19*, 20-25.
11. Nieuwoudt, M.K.; Shahlori, R.; Naot, D.; Patel, R.; Holtkamp, H.; Aguergaray, C.; Watson, M.; Musson, D.; Brown, C.; Dalbeth, N.; Cornish, J.; Simpson, M.C. Raman spectroscopy reveals age- and sex-related differences in cortical bone from people with osteoarthritis. *Sci. Rep.* **2020**, *10***,** 19443.
12. Gomez-Alonso, S.; Garcia-Romero, E.; Hermosin-Gutierrez, I. HPLC analysis of diverse grape and wine phenolics using direct injection and multidetecion by DAD and fluorescence. *J. Food Comp. Anal.* **2007**, *20*, 618-626.
13. Aleixandre-Tudo, J.L.; Buica, A.; Nieuwoudt, H.; Aleixandre, J.L.; Toit W. Spectrophotometric analysis of phenolic compounds in grapes and wines. *J. Ag. Food Chem.* **2017**, *65*, 4009-4026.
14. Chase, D.B. Fourier transform Raman spectroscopy. *J. Am. Chem. Soc*. **1986**, *108*, 7485-7488.
15. Ranatunge, I.; Adikary, S.; Dasanayake, P.; Fernando, C.D.; Soysa, P. Development of a rapid and simple method to remove polyphenols from plant extracts. *Int. J. Anal. Chem.* **2017**, *2017*, 1-7.
16. Mattick, L.R.; Rice, A.C. The use of PVPP of decolorizing wine in the determination of tartrate by metavanadate method. *Am. J. Enol. Vit.* **1981**, *32*, 297-298.

17. Rodriguez, S.B.; Thornton, M.A.; Thornton, R.J. Raman Spectroscopy and chemometrics for identification and strain discrimination of the wine spoilage yeasts *Saccharomyces cerevisiae*, *Zygosaccharomyces bailii*, and *Brettanomyces bruxellensis*. *App. Environ. Micro.* **2013**, *79*, 6264–70.
18. Frausto-Reyes, C.; Medina-Gutierrez, C.; Sato-Berru, R.; Sahagun, LR. Qualitative study of ethanol content in tequila by Raman spectroscopy and principal components analysis. *Spectro Acta* A **2005**, *61*, 2657-2662.
19. Boyaci, I.H.; Genis, H.E.; Guven, B.; Tamer, U.; Alper, N. A novel method for quantification of ethanol and methanol in distilled alcoholic beverages using Raman spectroscopy: Simultaneous detection of ethanol and methanol. *J. Raman Spect.* **2012** *43*, 1171–76.
20. Delfino, I.; Camerlingo, C.; Portaccio, M; Ventura, B.D.; Mita, L.; Mita, D.G.; Lepore, M. Visible micro-Raman spectroscopy for determining glucose content in beverage industry. *Food Chem*. **2011**, *127*, 735–42.
21. Richardson, P.I.C.; Muhamadali, H.; Ellis, D.I.; Goodacre, R. Rapid Quantification of the adulteration of fresh coconut water by dilution and sugars using Raman spectroscopy and chemometrics. *Food Chem.* **2019**, *272*, 157–64.
22. Pompeu, D.R.; Larondelle, Y.; Rogez, H.; Abbas, O.; Pierna, J.A.F.; Baeten, V. Characterization and discrimination of phenolic compounds using fourier transform Raman spectroscopy and chemometric tools. *Biotechnol. Agron.Soc. Environ.* **2018**, *22*, 13-28.
23. Wu, Z.; Xu, E.; Long, J.; Pan, X.; Xu, X.; Jin, Z.; Jiao, A. Comparison between ATR-IR, Raman, concatenated ATR-IR and Raman spectroscopy for the determination of total antioxidant capacity and total phenolic content of Chinese rice wine. *Food Chem.* **2016**, *194*, 671–79.

24. Wang, Q.; Li, Z.; Ma, Z.; Liang, L. Real time monitoring of multiple components in wine fermentation using an on-line auto-calibration Raman spectroscopy. *Sens. Actuat. B* **2014**, *202*, 426–32.
25. Ramírez-Elías, M.G.; Guevara, E.; Zamora-Pedraza, C.; Rogelio Aguirre, J.R.; Juárez, B.I.F.; Bárcenas-Pezos, G, M.; Ruiz, F.; González, F.J. Assessment of mezcal aging combining Raman spectroscopy and multivariate analysis. *Tech. Biomed. Spec. and Image* **2017**, *6*, 75–81.
26. Magdas, D.A.; Guyon, F.; Feher, I.; Pinzaru, S.C. Wine Discrimination based on chemometric analysis of untargeted markers using FT-Raman spectroscopy. *Food Control* **2018**, *85*, 385–91.
27. Teixera dos Santos, C.A.; Pascoa, R.N.M.J.; Porto, P.A.L.S.; Cerdeira, A.L.; Gonzalez-Saiz, J.M.; Pizarro, C.; Lopes, J.A. Raman spectroscopy for wine analysis: a comparison with near and mid infrared spectroscopy. *Talanta* **2018**, *186*, 306-314.
28. Pierna, J.A.F.; Abbas, O.; Dardenne, P.; Baeten. V. Discrimination of Corsican honey by FT-Raman spectroscopy and chemometrics. *Biotechnol. Agron. Soc. Environ.* **2011**, *15*, 75-84.
29. Agati, G.; Matteini, P.; Oliveira, J.; de Freitas, V.; Mateus, N. Fluorescence approach for measuring anthocyanins and derived pigments in red wine. *J. Ag. Food Chem.* **2013**, *61*, 10156-10162.
30. Poustka, F.; Irani, N.G.; Feller, A.; Lu, Y.; Pourcel, L.; Frame, K.; Grotewold, E. Trafficking pathway for anthocyanins overlaps with the endoplasmic reticulum-to-vacuole protein-sorting route in Arabidopsis and continues to the formation of vacuolar inclusions. *Plant Phys.* **2007**, *145*, 1323-1335.
31. Somers, T.C. The polymeric nature of wine pigments. *Phytochemistry* **1971**, *10*, 2175-2186.
32. Fe, H.; Na-na, L.; Duan, C.Q. Anthocyanins and their variation in red wines II: anthocyanin derived pigments and their color evolution. *Molecules*, **2012,** *17*, 1483-1519.

33. Lackey, H.E.; Nelson, G.L.; Lines, A.M.; Bryan, S.A. Reimagining pH measurements; utilizing Raman spectroscopy for enhanced accuracy in phosphoric acid systems. *Anal. Chem.* **2020**, *92*, 5882-5889.
34. Fu Q.; Wang, J.; Lin, G.; Suo, H.; Zhao, C. Short-wave near-infrared spectrometer for alcohol determination and temperature correction. J Anal Methods Chem **2012**, *2012*, 1-7.